

# Compact Ka-Band Phase Shifters Using MEMS Capacitive Switches

Cristiano Palego<sup>#1</sup>, Zhen Peng<sup>#</sup>, James C. M. Hwang<sup>#</sup>, Derek Scarbrough<sup>\*</sup>, David I. Forehand<sup>\*</sup> and Charles L. Goldsmith<sup>\*</sup>

<sup>#</sup>ECE, Lehigh University, 5 East Packer Ave, Bethlehem PA, 18015, USA

<sup>1</sup>crp207@lehigh.edu

<sup>\*</sup>MEMtronics Corp., Plano, TX 75075, USA

**Abstract** — This paper presents the design of a Ka-band phase shifter comprising a slow-wave structure that tightly wraps around three closely spaced MEMS capacitive switches. The switches are of proven design and reliability, except some switches have a gap in their stationary electrodes. This novel feature has negligible effect on electromechanical operation but provides another degree of freedom for simultaneous optimization of phase shift and impedance match. The design principle is validated through specially designed thin-film test structures. The results suggest that the present design is applicable to phase shifters of different sizes and resolutions with high performance, yield and reliability, but low cost and power consumption.

**Index Terms** — Microelectromechanical devices, microwave phase shifters, microwave switches, slow wave structures, transmission line theory.

## I. INTRODUCTION

Over the past decade, micro-electromechanical systems (MEMS) phase shifters have been intensively investigated for applications in phased-array radar and communications systems. Phase shifters based on periodic loading of a transmission line with MEMS capacitive switches have achieved large phase shift and low insertion loss from Ka to W band [1]. The phase shift is achieved by turning on the capacitive switches, which increases unit-length capacitance  $C$  of the line without significantly affecting its unit-length inductance  $L$ . This results in higher phase constant  $\beta = \omega\sqrt{LC}$  but lower characteristic impedance  $Z_0 = \sqrt{L/C}$ , where  $\omega$  is the angular frequency. Therefore, it is challenging for capacitively loaded MEMS phase shifters to maintain impedance match in both through (switches off) and delayed (switches on) states. Another consideration for the relatively new MEMS technology is the number of switches used, which can adversely impact yield and reliability.

Recently, a new phase shifter consisting of cascaded transmission line sections was proposed [2]. Using five MEMS ohmic (as opposed to capacitive) switches for each section, its capacitance and inductance can be increased simultaneously at a constant ratio, thereby achieving large phase shift without affecting impedance match. Impressive figures of merit such as  $257^\circ$  of phase shift per dB of insertion loss and  $> 19$  dB return loss in both through and delayed states were demonstrated up to 50 GHz. However, in

spite of the high-resistance bias lines used, each ohmic switch can consume on the order of 100 mW standby power, which reduces the advantage of the phase shifter over conventional phase shifters that are based on diodes or transistors.

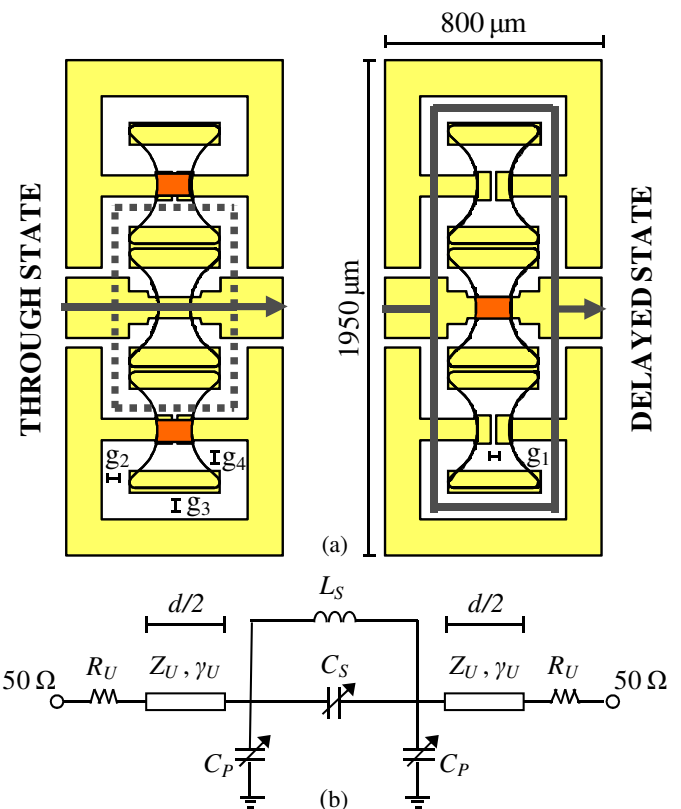


Fig. 1. (a) Layout and (b) equivalent circuit of a phase-shifter unit cell comprising a slow-wave structure tightly wrapped around three closely spaced MEMS capacitive switches. The movable electrode of each switch is made transparent to reveal the stationary electrode underneath. Darkened patch in the middle of the movable electrode indicates that it is pulled in to contact the stationary electrode. The stationary electrodes of the side switches have a gap  $g_1$  in the middle to allow independent optimization of phase shift and impedance match. The layout is duplicated to indicate the signal paths in both through and delayed states.

This paper presents a similar phase shifter design to that of [2], but with each section utilizing only three MEMS capacitive switches of negligible standby power but proven

TABLE I  
DERIVED/OPTIMIZED EQUIVALENT-CIRCUIT ELEMENTS

Element	45° Unit Cell		90° Unit Cell	
	Through	Delayed	Through	Delayed
$Z_U (\Omega)$	66/66	67/66	66/66	67/66
$\gamma_U d (^\circ)$	38/38	38/38	38/38	38/38
$R_U (\Omega)$	0.7/0.5	0.4/0.5	0.8/0.6	0.7/0.6
$C_P$ (fF)	17/18	80/80	14/15	116/115
$C_S$ (fF)	994/990	39/40	995/995	32/31
$L_S$ (pH)	249/250	245/250	284/285	288/285

reliability [3]. Furthermore, a simple equivalent circuit is used to represent the transmission line section in both through and delayed states. A rigorous analysis is used to solve the cascade (ABCD) matrix of the equivalent circuit for simultaneously optimization of the phase shift and impedance match. The proposed phase-shifter unit cell has been optimized for operation between 24.5 and 27 GHz with 45° phase shift, < 0.2 dB insertion loss, and > 20 dB return loss. By cascading the 45° unit cell with 90° unit cells of similar design, a 3-bit phase shifter is proposed with a phase shift vs. insertion loss ratio comparable to that of [2] but with fewer switches. The design principle is validated through specially designed thin-film test structures as described below.

## II. DESIGN PRINCIPLE AND MODELING

Fig. 1(a) shows that the phase-shifter unit cell is based on an  $800 \mu\text{m} \times 1950 \mu\text{m}$  slow-wave structure that tightly wraps around three closely spaced MEMS capacitive switches. Each switch includes a movable electrode and a stationary electrode. The stationary electrode is covered by a thin layer of dielectric, so that when the movable electrode is pulled in to contact the stationary electrode, a high-resistance high-capacitance contact is made. In the through state of the unit cell, the center switch is off (with the movable electrode suspended above the stationary electrode), while the side switches are on (with the movable electrode pulled in to contact the stationary electrode). In this case, most of the RF signal passes directly under the movable electrode of the center switch, while a small fraction of the signal detours along the stationary electrodes of the side switches (dotted line in Fig. 1). This adds some slow-wave characteristic to the through state and limits the phase shift between through and delayed states.

In the delayed state, the center switch is on while the side switches are off. The stationary electrodes of the side switches have a gap in the middle, which allows the signal to be routed around the side switches for a phase shift with respect to that of the through state. In addition, the gap affords more design freedom through the switchable series capacitance  $C_S$  as discussed next. The gap has negligible effect on the electromechanical operation of the switch.

The design principle of the above-described phase shifter is best understood through an equivalent circuit as shown in Fig.

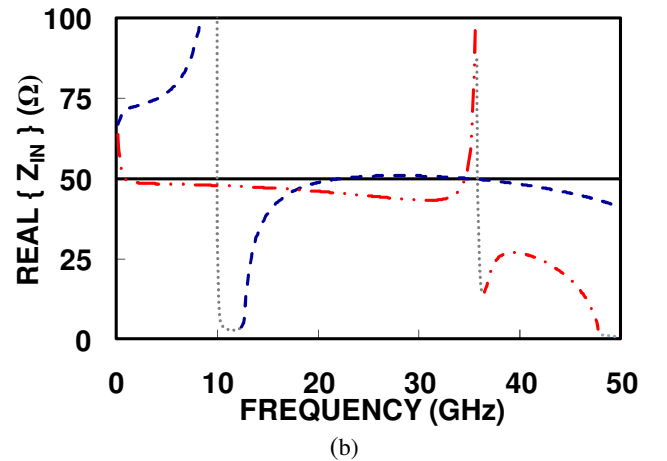
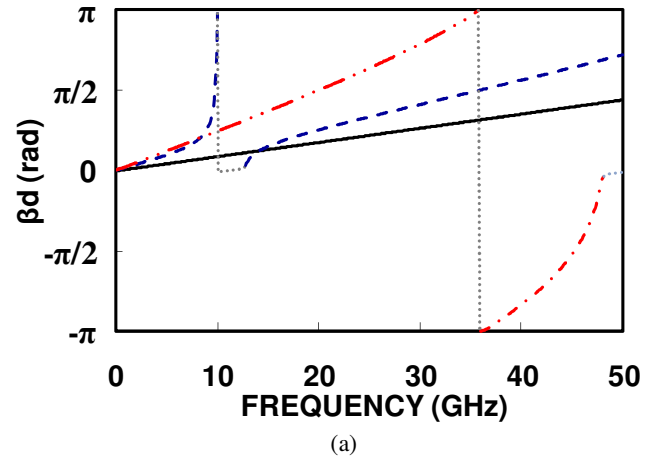


Fig. 2. (a) Imaginary part of propagation constant and (b) real part of input impedance of the 45° unit cell, including that of forward wave in through state (---), forward wave in delayed state (— · —), backward wave in delayed state (— ·), and a coplanar quasi-TEM transmission line (—).

1(b). The equivalent circuit contains a lumped section sandwiched between two distributed sections. The distributed sections have fixed impedance to account for the access lines with characteristic impedance  $Z_U$ , propagation constant  $\gamma_U$ , and physical length  $d/2$ . The line and switch losses are lumped into a series resistance  $R_U$ . The  $\Pi$ -shaped lumped section is purely reactive with its reactance switchable between through and delayed states. The parallel capacitors  $C_P$  accounts for the capacitance between the movable and stationary electrodes, as well as the fringing capacitance between the movable electrode and the surrounding ground plane of the slow-wave structure.  $L_S$  accounts for the series inductance of the lumped section including the discontinuity at the adjoining distributed sections.

The switchable elements of the lumped section can be simultaneously optimized to provide large phase shift but constant impedance in both through and delayed states. The series capacitance  $C_S$  affords another degree of freedom over the conventional topology of series  $L_S$  and shunt  $C_P$ . With the  $C_S/L_S$  resonance around 10 GHz,  $C_S$  tends to short out  $L_S$  in

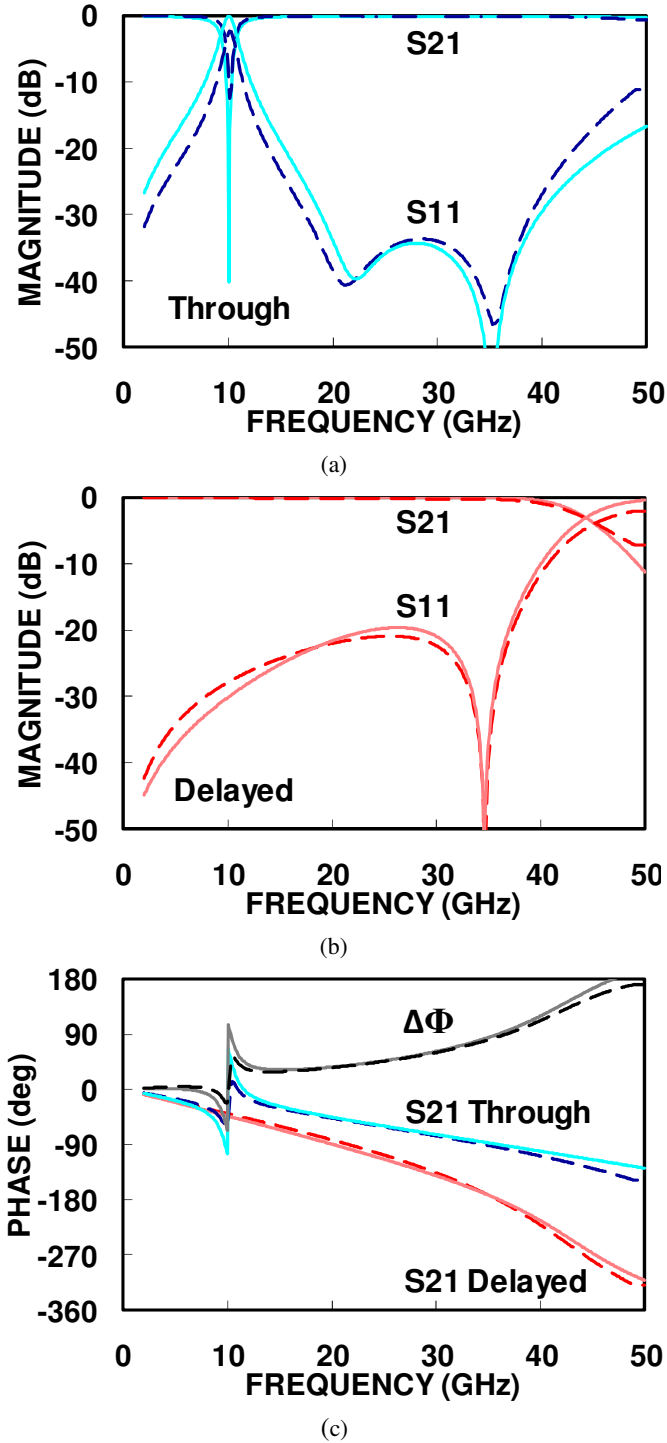


Fig. 3. Derived (solid) vs. optimized (dashed)  $S$ -parameter (a) magnitude in through state, (b) magnitude in delayed state, and (c) phase in both states of the  $45^\circ$  unit cell.

the though state over the frequencies of interest. In the delayed state,  $C_S$  decreases substantially while  $L_S$  is approximately constant. Therefore, the  $C_S/L_S$  reactance becomes inductive, which, together with the much increased  $C_P$  in the delayed state, results in large phase shift while maintaining good impedance match.

By simultaneously solving for the propagation constant and input impedance of the equivalent circuit, the optimum phase shift and impedance match can be derived. Table I shows that the derived and optimized equivalent-circuit elements are very close to each other. Details of the optimization through full-wave simulation are discussed in the next section.

### III. DESIGN OPTIMIZATION AND SIMULATION

The derived equivalent circuit has been implemented on a quartz substrate with  $635 \mu\text{m}$  thickness, 3.79 dielectric constant, and 0.0004 loss tangent. Except for the gap  $g_1$  in the stationary electrode, the MEMS switches are exactly the same as in [3] with on and off capacitances of approximately 1 pF and 35 fF, respectively. Other than the switches, the only layout parameters that need to be optimized are the gaps between the switches and the surrounding ground plane. As indicated in Fig. 1,  $g_1$  affects mainly  $C_S$ ,  $g_2$  and  $g_3$  affect mainly  $C_P$ , while  $g_4$  controls the return loss.

Full-wave simulation by Agilent's MOMENTUM was used for further optimization of the layout. Fig. 2 plots the optimized propagation constant and input impedance of the  $45^\circ$  unit cell. As expected, in the through state and except around 10 GHz, the propagation constant is mostly imaginary with a small real part due to  $R_U$ . The propagation constant in the delayed state exhibits also a backward wave above 35 GHz where  $\beta < 0$  while the group velocity  $d\omega/d\beta > 0$ . The slow-wave factor was evaluated as the ratio of the unit-cell propagation constant and that of a  $50 \Omega$  coplanar quasi-TEM transmission line on the same substrate. At the center frequency of 25.75 GHz, the ratios were 1.6 and 2.8 for the through and delayed states, respectively. The input impedance was mostly real in the pass bands and close to  $50 \Omega$  for both states. At 25.75 GHz, the input impedance was 50.8 and 45.1  $\Omega$  for the through and delayed states, respectively.

Fig. 3 shows that the simulated phase shift of  $48^\circ$  at 25.75 GHz is within 5% of the value derived from the equivalent circuit. The return loss is better than 20 dB in both states from DC to 35 GHz, except around the 10 GHz resonance in the through state. The worst insertion loss in the band of interest is 0.19 dB in the delayed state. The figures of merit are  $253^\circ/\text{dB}$  and  $60^\circ/\text{mm}$  at 25.75 GHz.

### IV. EXPERIMENTAL VALIDATION

For low-cost expedient proof of the concept, two thin-film test structures without MEMS switches were designed to emulate the unit cell in both through and delayed states. A DC short is used to emulate the RF short between the movable and stationary electrodes when a switch is on, whereas an interdigitated capacitor is used to emulate the fringing capacitance between the electrodes when the switch is off. Thus, except somewhat worse return loss in the through state, the test structures have comparable phase shifts and losses as the MEMS implementation. Fig. 4 illustrates the fabricated

## V. 90° UNIT CELL AND 3-BIT PHASE SHIFTER

A 90° unit cell was designed with moderate changes in the  $g_1$ - $g_4$  gaps and the coplanar line configuration resulting in an  $800 \mu\text{m} \times 2350 \mu\text{m}$  slow-wave structure. The corresponding equivalent-circuit elements have been listed in Table I along with that of the 45° unit cell. The optimized 90° unit cell has 94° phase shift, 0.27 dB insertion loss, and > 20 dB return loss at 25.75 GHz. The corresponding figures of merits are 350°/dB and 120°/mm. Similar to the case of the 45° unit cell, performance measured on 90° thin-film test structures agree with that simulated.

Three 90° unit cells can be cascaded with a 45° unit cell to form a 3-bit phase shifter. With all unit cells in the delayed state, the simulated phase shift is 330° while the simulated insertion loss is less than 1 dB at 25.75 GHz. The return loss is greater than 21 dB between dc and 25 GHz. The results suggest that the present design is applicable to phase shifters of different sizes and resolutions with high performance, yield and reliability, but low cost and power consumption.

## VI. CONCLUSION

This paper presents the design of a Ka-band phase shifter incorporating a minimum number of MEMS capacitive switches of proven design and reliability into a compact slow-wave structure. Some of the switches contain a novel gap in their stationary electrodes to allow for simultaneous optimization of phase shift and impedance match. The design principle is confirmed through full-wave simulation and validated through thin-film test structures. The results suggest that 3-bit Ka-band phase shifters with less than 1 dB of insertion loss and greater than 20 dB of return loss are realizable by using the present technology and design.

## ACKNOWLEDGEMENT

This work is supported in part by the NASA Jet Propulsion Laboratory under STTR Contract No. NNX08CD55P.

## REFERENCES

- [1] N. S. Barker, and G. M. Rebeiz, "Optimization of distributed MEMS transmission-line phase shifters—U-band and W-band designs," *IEEE Trans. Microwave Theory Techniques*, vol. 48, pp. 1957-1966, Nov 2000.
- [2] B. Lakshminarayanan, and T. M. Weller, "Design and modeling of a 4-bit slow-wave MEMS phase shifter," *IEEE Trans. Microwave Theory Techniques*, vol. 54, pp. 120-127, Jan. 2006.
- [3] C. L. Goldsmith, D. I. Forehand, Z. Peng, J. C. M. Hwang, and J. L. Ebel, "High-cycle life testing of RF MEMS switches," *IEEE MTT-S Int. Microwave Symp. Dig.*, pp. 1805-1808, June 2007.

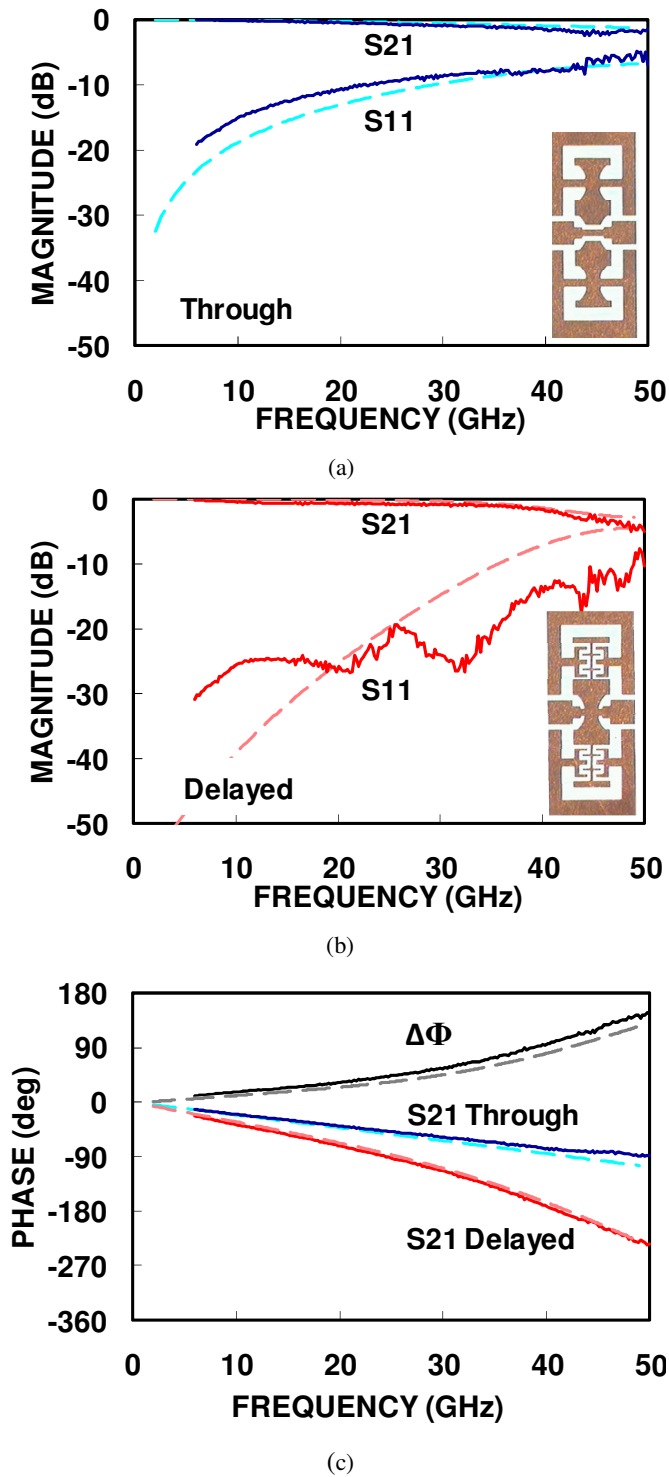


Fig. 4. Measured (solid) vs. simulated (dashed)  $S$ -parameter (a) magnitude in through state, (b) magnitude in delayed state, and (c) phase in both states of thin-film test structures that emulate the through and delayed states, respectively, of the 45° unit cell.

structures and test results. In both the through and delayed states, the insertion loss is better than 0.47 dB and in agreement with simulation. The measured phase shift at 25.75 GHz is 44°.